LETTER

Ammonia-Mediated CO_2 Capture and Direct Electroreduction to Formate

Hengzhou Liu, Yifu Chen, Jungkuk Lee, Shuang Gu, and Wenzhen Li*

Read Online

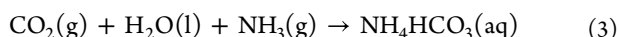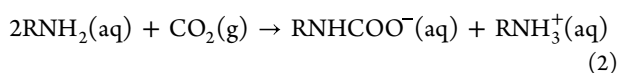ACCESS | 📊 Metrics & More | 📰 Article Recommendations | 🆂🅸 Supporting Information

ABSTRACT: Direct electrochemical conversion of CO_2 capture solutions (instead of gaseous CO_2) to valuable chemicals can circumvent the energy-intensive CO_2 regeneration and pressurization steps, but the performance of such processes is limited by the sluggish release of CO_2 and the use of energy-consuming bipolar membranes (BPMs). Herein, we discovered that an ammonium bicarbonate (NH_4HCO_3)-fed electrolyzer outperforms the state-of-the-art $KHCO_3$ electrolyzers largely because of its favorable thermal decomposition property, which allows for a 3-fold increase in the *in situ* CO_2 concentration, a maximum 23% increase in formate faradaic efficiency, and a 35% reduction in cell voltage by substituting BPM with an anion exchange membrane (AEM). We then demonstrated an integrated process by combining NH_4HCO_3 electrolysis with CO_2 capture by on-site generated ammonia from the electroreduction of nitrate, which features a remarkable 99.8% utilization of of CO_2 capturing agent. Such a multipurpose process offers a sustainable route for the simultaneous removal of N wastes and streamlined CO_2 capturing and upgrading.
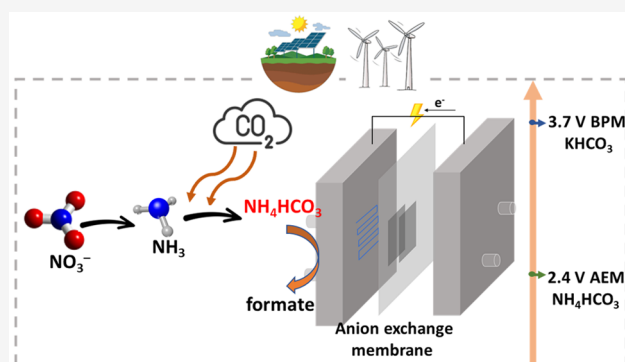
Reduction of the net CO_2 emissions to zero by 2050 is an urgent need for limiting global warming to a safe level.[1−4] Powered by renewable electricity from solar or wind sources, CO_2 can be electrochemically converted into valuable chemicals and fuels (i.e., the CO_2 reduction reaction, or CO2RR).[1,5] However, CO_2 electrolyzers in most studies are fed with pressurized and purified CO_2 gas, production of which requires energy- and capital-intensive regeneration processes from the captured CO_2.[6,7] Specifically, after capturing CO_2 from air or flue gases, the release of CO_2 is usually accomplished by heating the capturing media at 120−150 °C.[8,9] Then, the collected CO_2 must be compressed into a pressurized container for storage and transportation before its utilization. Therefore, integrating CO_2 capture and conversion steps is vital to decreasing the energy costs and making the overall process sustainable.[7,10]
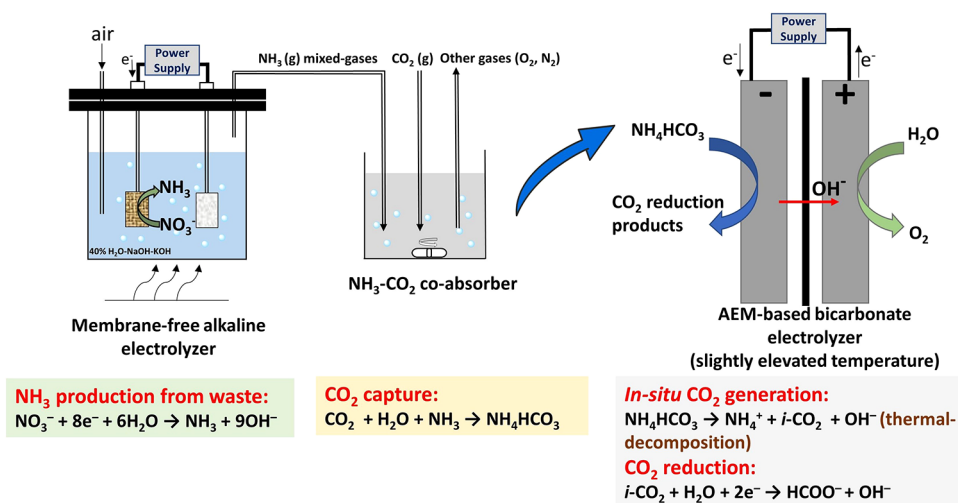
$$KOH(aq) + CO_{2(g)} \rightarrow KHCO_3(aq) \quad (1)$$

$$2RNH_2(aq) + CO_2(g) \rightarrow RNHCOO^-(aq) + RNH_3^+(aq) \quad (2)$$

$$CO_2(g) + H_2O(l) + NH_3(g) \rightarrow NH_4HCO_3(aq) \quad (3)$$

One strategy is to convert CO_2 directly in its capture solutions upon its *in situ* release.[7] In bipolar membrane (BPM)-based electrolyzers, aqueous bicarbonate—generated by absorbing CO_2 in KOH capture solution (RXN 1)—can

react with H^+ produced by the BPM to form *in situ* CO_2 (*i*-CO_2) at the BPM-electrode interface (RXN 4), which can be subsequently converted into value-added products such as CO,[11−15] formate,[16] and CH_4.[17] However, the performance of such bicarbonate electrolyzers is inferior to direct CO_2 electrolyzers fed with gaseous CO_2, largely due to the inadequate local *i*-CO_2 concentration.[18,19] Besides, the metal cation bicarbonate electrolyzer has significantly higher electrical energy consumption, because the BPM requires an additional potential of 0.828 V (under standard conditions) for H^+ generation by water dissociation upon large current densities,[15] and BPM is thicker than conventional cation and anion exchange membranes (CEM and AEM).

Apart from the KOH solution, amines such as monoethanolamine (MEA) solution are commonly used for capturing CO_2 due to the facile kinetics of the formation of amine-CO_2 adducts (RXN 2).[20−22] Conversion of the MEA-CO_2 adduct to CO has been reported in previous studies but only at low current densities (<50 mA cm^{-2}).[20,21,23] In addition to the

Scheme 1. Schematic Illustration of the Integrated Process of CO_2 Capture and Utilization[a]

NH$_3$ production from waste:
$NO_3^- + 8e^- + 6H_2O \rightarrow NH_3 + 9OH^-$

CO_2 capture:
$CO_2 + H_2O + NH_3 \rightarrow NH_4HCO_3$

In-situ CO_2 generation:
$NH_4HCO_3 \rightarrow NH_4^+ + i\text{-}CO_2 + OH^-$ (thermal-decomposition)

CO_2 reduction:
$i\text{-}CO_2 + H_2O + 2e^- \rightarrow HCOO^- + OH^-$

[a]This process combines NH_3 production from NO_3^-, waste CO_2 capture by coabsorption with NH_3, and production of value-added commodity chemicals from the bicarbonate electrolyzers. In the NO_3^- electrolyzer, the air was used as the carrier gas to purge NH_3-containing gases out of the reactor for its further capture of CO_2 in water: acid−base reaction between NH_3 and CO_2 ($NH_3 + CO_2 + H_2O \rightarrow NH_4HCO_3$).
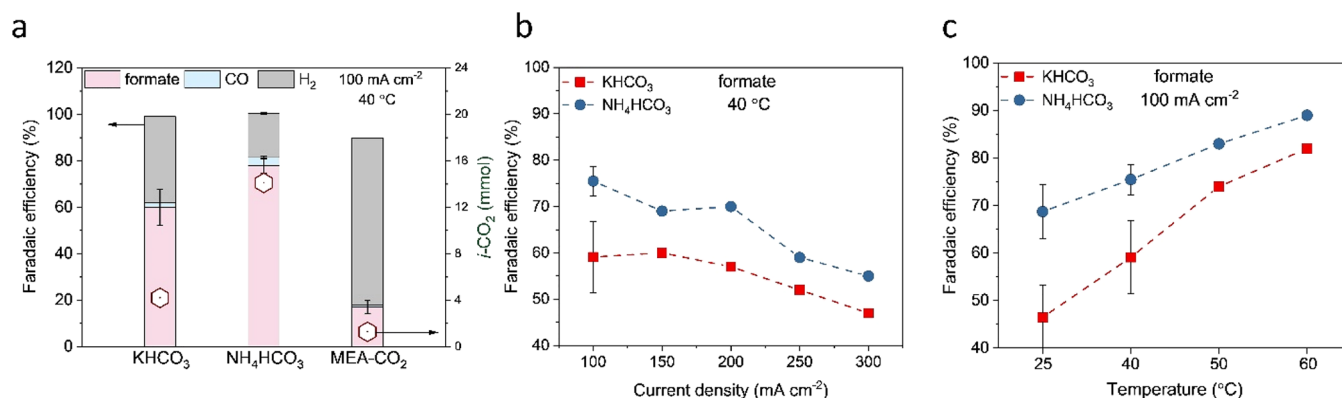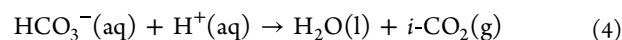

Figure 1. Electrochemical conversion of CO_2 capture solutions to formate. (a) Faradaic efficiency (left Y-axis) of products and the amount of *in situ* generated CO_2 (right Y-axis) during the electrolysis of different CO_2 capture solutions (2.5 M for all cases): $KHCO_3$, NH_4HCO_3, and MEA-CO_2. The electrolysis was performed at 40 °C for 30 min at a constant current density of 100 mA cm^{-2}. The MEA-CO_2 adduct was prepared by bubbling CO_2 for 30 min into the solution of MEA and then purging argon to remove dissolved CO_2. 2.5 M KCl was added to the MEA-CO_2 solution to increase its conductivity.[20] Comparison of formate faradaic efficiency with $KHCO_3$ and NH_4HCO_3 at (b) different current densities and (c) different cell temperatures during 30 min electrolysis. The catholyte volume was 40 mL for 100−150 mA cm^{-2} and 120 mL for 200−300 mA cm^{-2}, respectively.

insufficient *i*-CO_2 concentration, the bulky carbamate ($RNHCOO^-$) and ethanolammonium (RNH_3^+) ions may hinder the mass transport at the electrode double layer, which limits the *i*-CO2RR performance.

As a suitable alternative, CO_2 can be captured by ammonium (NH_4^+) solution to form ammonia bicarbonate (NH_4HCO_3) (RXN 3).[23,24] Compared to MEA, NH_3 has a higher CO_2-capturing capacity because it doubles the stoichiometric ratio of CO_2 to the capturing agent (RXN 2 and 3).[25] More importantly, release of CO_2 from NH_4HCO_3 requires much lower energy than that from MEA-CO_2 or $KHCO_3$, as illustrated by their decomposition temperatures: 36, 120, and 150 °C for NH_4HCO_3, MEA-CO_2, and $KHCO_3$, respectively.[26] The ease of CO_2 release from NH_4HCO_3 (RXN 5) is expected to provide sufficient *i*-CO_2 in the electrolyzer and facilitate *i*-CO2RR with reduced energy input. Besides, the cost of NH_3 (13.5 USD per kmol[27]) is much lower than that of KOH (86 USD per kmol[28]) or MEA (92 USD per kmol[29]),

and NH_3 as the CO_2 capture agent is less corrosive and less toxic as compared to KOH,[26] as shown in Supporting Information Note 1. Moreover, NH_3 can be readily produced by the electroreduction of NO_x or NO_x^- that is abundant in agricultural or industrial wastes.[30−33] Using waste-derived NH_3 for CO_2 capture and conversion will simultaneously alleviate the environmental burdens of NO_x/NO_x^- and CO_2 by "fixing" them into stable and value-added chemical products (Scheme 1).[34,35]

Conventional work: water dissociation driven in BPM electrolyzer

$$HCO_3^-(aq) + H^+(aq) \rightarrow H_2O(l) + i\text{-}CO_2(g) \tag{4}$$

This work: thermal decomposition driven in AEM electrolyzer

$$NH_4HCO_3(aq) \rightarrow NH_4^+(aq) + i\text{-}CO_2(g) + OH^-(aq) \tag{5}$$
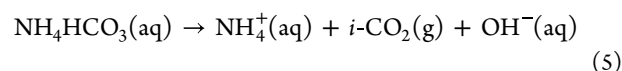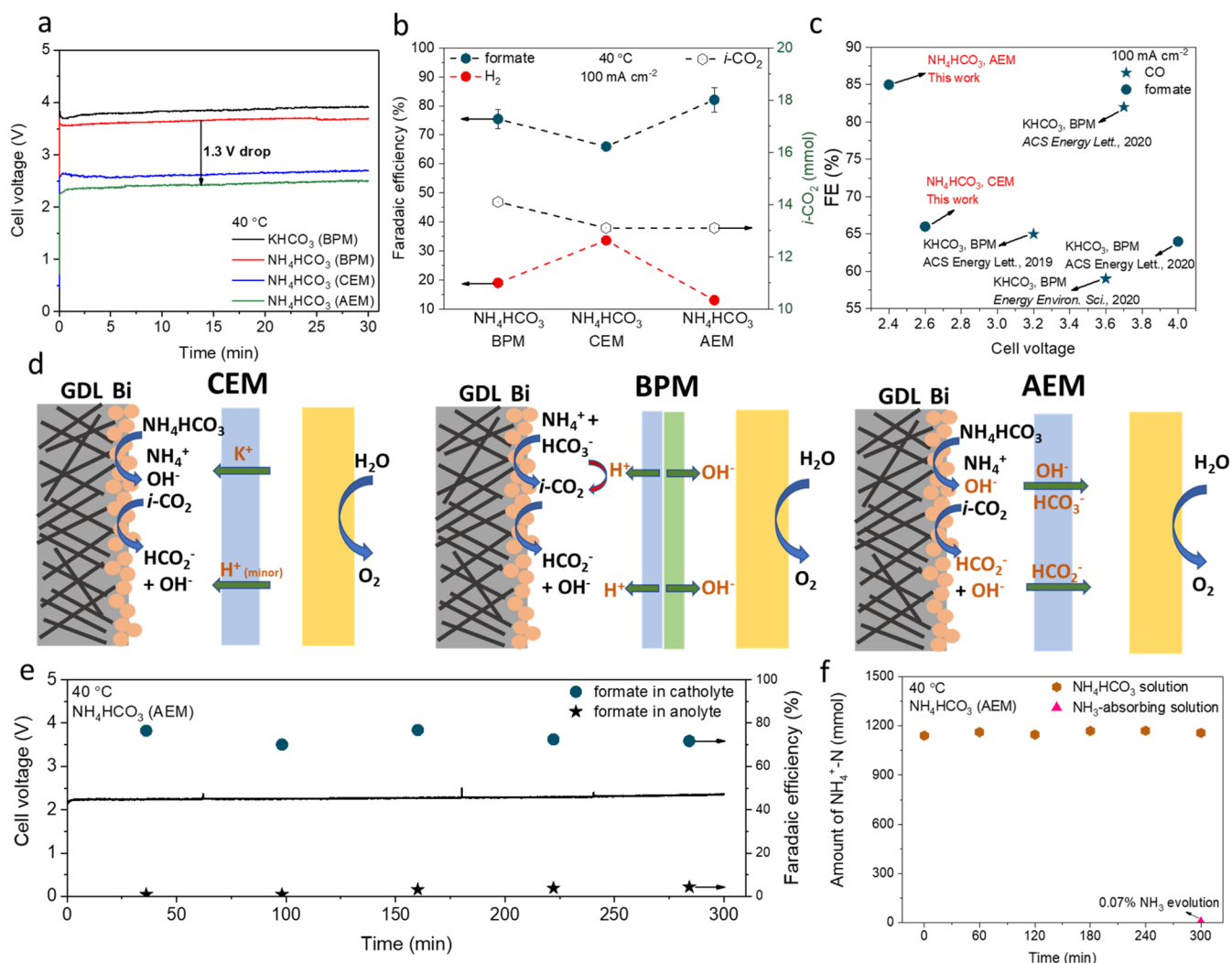
Figure 2. Conversion of NH_4HCO_3 in the electrolyzers with different membranes. (a) Cell voltage profile and (b) faradaic efficiency (left Y-axis) of products and the amount of *in situ* generated CO_2 (right Y-axis) for the electrolysis of $KHCO_3$ and NH_4HCO_3 with different membranes: BPM, CEM, and AEM. The electrolysis was performed at 40 °C for 30 min at a constant current density of 100 mA cm^{-2}. (c) Comparison of the cell voltage and the FE toward product (formate) in this work with the reported performances[11,12,16,44] using $KHCO_3$ and BPM at 100 mA cm^{-2}. (d) Schematic illustration of the local environment at the cathode for the electrolyzers with NH_4HCO_3 feed when using different membranes. (e) Cell voltage profile and formate faradaic efficiency (for both catholyte and anolyte) for 5 h electrolysis in an AEM-based system at a cell temperature of 40 °C. (f) Amount of NH_4^+ in the NH_4HCO_3 solution and the acid absorbing solution.

One known obstacle to using NH_3 as the capture agent is its volatility, and it may escape from NH_3 solution during capture operation and handling.[26] Through system modeling and optimization, such as the advanced flash stripper process,[36,37] both operational and economic feasibilities have been demonstrated for NH_3-based CO_2 capture (chilled NH_3 process)[38,39] from postcombustion streams. For example, a proposed two-stage adsorption process has reduced NH_3 slip by more than 50%, leading to the recovery of >99% of vaporized NH_3.[40] The CO_2-avoided cost has been reduced to US$ 40.7/ton CO_2 for NH_3-based CO_2 capture, which is 44% less than the MEA-based process (US$ 75.1/ton CO_2).[36] Albeit the successful modeling of the capability of using NH_3 as the capture agent, the utilization of CO_2 captured media—the direct conversion of NH_4HCO_3 solution in the electrolyzers—has never been developed. Besides, the previous studies were limited to theoretically modeling the technical and economic capability of NH_3-based CO_2 capture. A combined process for NH_3-mediated CO_2 capture (with

NH_3 derived waste resources) and its direct utilization (conversion in electrolyzers) has not been achieved experimentally.

We first investigated the CO2RR performance in a BPM-based electrolyzer with NH_4HCO_3 as the electrolyte and reactant. Formate was chosen as the target CO2RR product in this study due to its known economic feasibility.[5,41] Besides, recent work has proposed that ammonium formate is a safe and energy-dense electrochemical fuel with an energy density of 3.2 kWh/L, higher than that of formic acid and hydrogen.[42] Electrodeposited bismuth (ED-Bi) on a carbon paper substrate was used as the CO2RR catalyst.[16] Scanning electron microscopy (SEM) images and an X-ray diffraction (XRD) pattern show the uniform deposition of metallic Bi on carbon paper (Figure S1). The electrolyzer with a zero-gap configuration consisted of the ED-Bi cathode, a BPM, and a piece of nickel foam as the anode. The catholyte and anolyte were supplied to their respective electrode compartment at an identical flow rate of 50 mL min^{-1}.

Figure 1a shows the comparison of i-CO2RR performance at 40 °C with three kinds of CO_2-capturing solutions (2.5 M for all cases): NH_4HCO_3, $KHCO_3$, and MEA-CO_2. At 100 mA cm^{-2}, the faradaic efficiency (FE) of formate production was 75 ± 3% for NH_4HCO_3, much higher than that of $KHCO_3$ (59 ± 7%) and MEA-CO_2 (18 ± 3%). The main side reaction was the hydrogen evolution reaction (HER), and the FE toward CO production was less than 2%. Interestingly, the trend of FE toward formate is consistent with the amount of generated i-CO_2, which was determined by summing the amounts of CO_2 (evolved from the catholyte and detected by gas chromatography) and CO2RR products generated during the electrolysis. The total i-CO_2 produced from NH_4HCO_3 was 3.4 or 10.8 times that of $KHCO_3$ or MEA-CO_2, respectively. The poor CO2RR performance with MEA-CO_2 could be attributed to the bulky ions of MEA-CO_2 that inhibit i-CO_2 formation and transportation.[23] Furthermore, by comparing the results with the corresponding control cells without applied current (Table S1), we found the portion of produced i-CO_2 from thermal decomposition was 93% for NH_4HCO_3, much higher than that for $KHCO_3$ (52%), highlighting the ease of CO_2 release from NH_4HCO_3.

The CO2RR performances of the systems with NH_4HCO_3 and $KHCO_3$ were further compared at different current densities ranging from 100 to 300 mA cm^{-2} (Figure 1b) and cell temperatures from 25 to 60 °C (Figure 1c). The system with NH_4HCO_3 shows 10−20% higher formate-oriented FE than $KHCO_3$ under all tested conditions. Limited by the mass transport i-CO_2, the remaining FE attributed to the competing H_2 (major) and CO (minor, <2%) evolutions, which exhibited an opposite trend as compared to formate formation (Figure S2 and Table S2). At 100 mA cm^{-2}, the highest formate FE was 90% with NH_4HCO_3 at 60 °C, which is higher than the reported values in the bicarbonate electrolyzers for formate production.[16,43]

Since the thermal decomposition dominates the production of i-CO_2 from NH_4HCO_3 (compared to the minor contribution from BPM), we further seek to remove the energy-consuming BPM in the electrolyzer to reduce the cell voltage. As shown in Figure 2a, substituting BPM with CEM or AEM indeed resulted in a decrease in the cell voltage from 3.7 to 2.4 V. Figure 2b compares the CO2RR performances with NH_4HCO_3 feed using BPM, CEM, and AEM as the membrane. The i-CO_2 production only decreased slightly as the BPM was replaced by CEM or AEM due to the absence of H^+ from BPM by water dissociation. In particular, when AEM is used, HER can be largely suppressed to 13% under a relatively high local pH (Figure 2d), resulting in a maximum formate FE of 82 ± 4% among the systems with three membranes. It is worth noting that we have taken into account the possible crossover of formate in three membrane cases, and the total FE is calculated by summing the formate concentration in both catholyte and anolyte. We did not observe any formate crossover in the CEM- or BPM-based eletrolyzer, and the percentage of its crossover in the AEM-based system was 4.7% (Table S3).

The above results demonstrate that replacing BPM with AEM for the NH_4HCO_3 electrolyzer not only reduces the energy consumption significantly but also increases the FE toward formate due to the favorable microenvironments at the electrode-membrane interface. The results are in stark contrast to the reported bicarbonate electrolyzer with $KHCO_3$ feed,[16] in which AEM showed a lower performance (<20% formate

FE) compared to BPM (62% formate FE): in that case, generation of i-CO_2 almost solely relies on the H^+ supply from the membrane owing to the sluggishness of the thermal decomposition of $KHCO_3$. As shown in Figure 2c, the performance of our NH_4HCO_3 electrolyzer is superior to the state-of-the-art bicarbonate electrolyzers in terms of cell voltage and FE.

To investigate the volatility of NH_3 in the NH_4HCO_3-based electrolyzer, we conducted 5 h electrolysis in the AEM-based system and quantified NH_3 loss during electrolysis (photo in Figure S3). In theory, in the aqueous electrolyte with buffered NH_4HCO_3 solution, NH_4^+ (aq) is the dominating species (detailed analysis in Supporting Information Note 2). We have experimentally tested the remained NH_4^+ (aq) and lost NH_3 (g) by NMR (details in the Experimental section 4.1). Indeed, at 100 mA cm^{-2}, negligible NH_3 loss was observed in the electrolyzer, since the amount of NH_4^+ (aq) was virtually unchanged in the NH_4HCO_3 solution at each hour interval and the escaped NH_3 was merely 0.07% (in NH_4^+ equivalent) among the total NH_4HCO_3 detected in the NH_3-absorbing solution (Figure 2f). A very stable cell voltage was observed at 2.2 V throughout the entire electrolysis, and the total formate FE (catholyte + anolyte) varied in a narrow range between 74 and 79% (Figure 2e), both of which indicate the stable operation of the NH_4HCO_3 electrolysis with AEM. We observed a slight increase in the crossover of formate to anolyte during the 5 h electrolysis. This was attributed to the gradual increase in the concentration gradient of formate between the catholyte and anolyte. Even so, the total crossover was still <5% after 5 h. The SEM image (Figure S4) showed that the Bi catalyst maintained a nanosized structure, where the morphology of nanosheets was likely formed due to the in $situ$ transformation from Bi nanoparticles under the electrolysis conditions.[45,46]

To quantitatively compare the energy consumption of CO2RR in different cell configurations, we analyzed the contributions to energy consumption for formic acid production at the current density of 100 mA cm^{-2} (detailed calculation methods are described in the Supporting Information Note 3). As shown in Figure 3, for the systems with gaseous CO_2 feed (cases 1-i and 1-ii), the majority of energy consumption arises from the regeneration of CO_2, leading to higher total energy consumption than the systems fed with CO_2 capture solutions. Compared with other cases, conversion of MEA-CO_2 solution (case 2-ii) requires additional input of electrical energy owing to its low FE toward the desired product. The lowest energy consumption corresponded to the systems with NH_4HCO_3 feed following the order of AEM < CEM < BPM (cases 2-iii to 2-v), in accordance with our experimental data.

Apart from the ease of CO_2 release, another key advantage of NH_3-based CO_2 capture is that NH_3 can be sustainably produced from wastes. As NO_3^--N is a major form of pollutants in wastewater,[47] its electrochemical reduction offers a sustainable pathway to NH_3 as a waste-derived CO_2 capturing agent while alleviating the environmental impact of NO_3^- itself. For this purpose, we developed an integrated system consisting of an electrolyzer for NH_3 production and an absorbing unit for capturing CO_2 (Figure S5). The NH_3-producing electrolyzer was modified from the configuration in our previous work,[48] which contains a concentrated NaOH-KOH solution as the electrolyte and commercial nickel wire mesh as the electrode. The use of high alkalinity and elevated
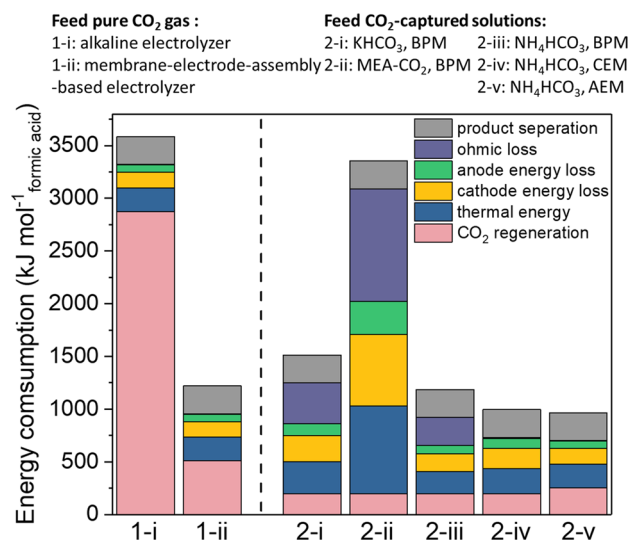
Figure 3. Analysis of the energy consumption for formic acid production from CO_2 electroreduction with different cell configurations. Cases 1-i and 1-ii correspond to the electrolyzers with gaseous CO_2 feed, and cases 2-i to 2-v correspond to the electrolyzers fed with CO_2 capture solutions.

temperature (80 °C) facilitated simultaneous NH_3 production and separation. NO_3^- reduction was performed under a continuous flow of N_2, which carries the produced NH_3 into a CO_2-saturated water solution cooled at 5 °C for NH_4HCO_3 formation.

Electrolysis was performed at 500 mA cm^{-2} for 6 h with the supply of theoretical charge of NO_3^--to-NH_3 reaction (Figure S6), yielding a NH_4HCO_3 solution with a concentration of 1.21 M in the integrated NO_3^--to-NH_4HCO_3 system. For NO_3^- electrolysis, Figure 4a showed the FE of NH_3 production was 99.5% with the nearly complete conversion of NO_3^- (98.8%), while the FE of the side-product NO_2^- was 0.06%. For the CO_2 capturing unit, only a trace amount of NH_3 evolution (0.2% of the total NH_3 generated) was detected from its outlet, suggesting the high utilization of NH_3 (99.8%) as the on-site generated CO_2 capturing agent. The low boiling

point (−33.34 °C) of ammonia and its high vapor pressure in the alkaline environment as well as its high pK_a (acid−base reaction between NH_3 and CO_2 in water: $NH_3 + CO_2 + H_2O \rightarrow NH_4HCO_3$) have guaranteed the simultaneous NH_3 generation, separation, and CO_2 capturing.[49]

Further extending the electrolysis duration in a scaled-up reactor (see the details in the experimental section 3.2 and our recent work[50]) led to the precipitation of solid NH_4HCO_3. The crystal phase of the separated solid was confirmed by comparing the XRD pattern with the commercial NH_4HCO_3 product (Figure 4b). In the BPM-based bicarbonate electrolyzer, electrolysis with the as-prepared NH_4HCO_3 showed a formate FE of 70%, which is close to the result with commercial NH_4HCO_3 (FE: 79%) under identical conditions. The slightly lower performance is possibly because of its slightly lower NH_4HCO_3 (91.4%, determined by ^1H NMR spectroscopy as shown in Figure 4c) due to the incorporation of water during its precipitation. Such a tandem process can effectively "seal" the waste nitrogen and waste carbon into NH_4HCO_3 as a stable, pure, and easy-to-handle chemical product. Benefiting from the highly reversible nature of NH_4HCO_3 formation and decomposition, waste N-derived NH_3 can "shuttle" the waste CO_2 for its electrochemical conversion by the CO_2 capture-release cycling process.

In summary, our study demonstrated that NH_4HCO_3 can serve as a unique, highly reactive platform that bridges CO_2 capturing and its electrochemical conversion via its facile *in situ* release. In this regard, NH_4HCO_3 has shown enhanced CO2RR performance compared to $KHCO_3$ and MEA-CO_2, owing to its much lower energy requirement for releasing *i*-CO_2 within the elecrolyzer. A mildly elevated temperature (e.g., 40 °C) was proven sufficient for generating adequate *i*-CO_2 for its efficient electroreduction with negligible ammonia loss, lifting the requirement of the energy-consuming BPM in the cell system and thus providing a proper solution to the high cell voltage of the prevailing electrolyzers for CO_2 capture solutions. The ammonium formate product from such a highly selective process can be used as an appealing candidate as an energy carrier.[42] Further optimization of the electrode-membrane interface for enhanced CO2RR activity, development of the reabsorption process to recycle the unreacted *i*-
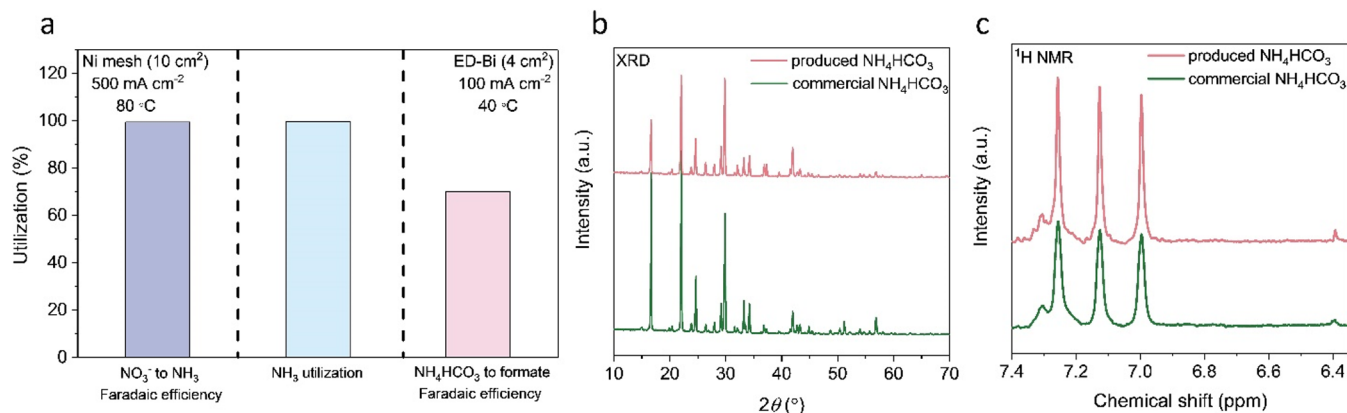

Figure 4. An integrated process combining CO_2 capture by NO_3^--derived NH_3 and formic acid production from NH_4HCO_3. (a) Utilization of the reaction ingredients for each individual process, including (1) electron utilization (faradaic efficiency) of the electrochemical NO_3^--to-NH_3 reaction; (2) utilization of the on-site generated CO_2 capturing agent (NH_3) for NH_4HCO_3 production; (3) electron utilization (faradaic efficiency) of the electrochemical formate production from the as-prepared NH_4HCO_3. The NH_4HCO_3 solution for electrolysis was prepared by dissolving 7.9 g of the NH_4HCO_3 (obtained by the reaction between NO_3^--derived NH_3 and CO_2) in 40 mL of deionized water. Comparison of the (b) XRD pattern and (c) ^1H NMR spectrum of the as-prepared NH_4HCO_3 and the commercial product.

CO_2 and NH_3 from the electrolyzer, and exploration of other CO2RR products beyond formate will bring exciting new opportunities for realizing the "waste-to-wealth" goal under the sustainable energy framework.

■ ASSOCIATED CONTENT

ⓈⒾ Supporting Information

The Supporting Information is available free of charge at https://pubs.acs.org/doi/10.1021/acsenergylett.2c02247.

> Experimental methods, structural/morphological characterization results, FE of products, and energy consumption estimations (PDF)

■ AUTHOR INFORMATION

Corresponding Author

Wenzhen Li − *Department of Chemical and Biological Engineering, Iowa State University, Ames, Iowa 50011, United States;* ⓞ orcid.org/0000-0002-1020-5187; Email: wzli@iastate.edu

Authors

Hengzhou Liu − *Department of Chemical and Biological Engineering, Iowa State University, Ames, Iowa 50011, United States*

Yifu Chen − *Department of Chemical and Biological Engineering, Iowa State University, Ames, Iowa 50011, United States*

Jungkuk Lee − *Department of Chemical and Biological Engineering, Iowa State University, Ames, Iowa 50011, United States*

Shuang Gu − *Department of Mechanical Engineering, Wichita State University, Wichita, Kansas 67260, United States;* ⓞ orcid.org/0000-0003-1532-0093

Complete contact information is available at:
https://pubs.acs.org/10.1021/acsenergylett.2c02247

Notes

The authors declare no competing financial interest.

■ REFERENCES

(1) Nitopi, S.; Bertheussen, E.; Scott, S. B.; Liu, X.; Engstfeld, A. K.; Horch, S.; Seger, B.; Stephens, I. E.; Chan, K.; Hahn, C.; et al. Progress and perspectives of electrochemical CO_2 reduction on copper in aqueous electrolyte. *Chem. Rev.* **2019**, *119* (12), 7610−7672.

(2) Pachauri, R. K.; Allen, M. R.; Barros, V. R.; Broome, J.; Cramer, W.; Christ, R.; Church, J. A.; Clarke, L.; Dahe, Q.; Dasgupta, P.; et al.*Climate change 2014: synthesis report. Contribution of Working Groups I, II and III to the fifth assessment report of the Intergovernmental Panel on Climate Change*; IPCC, 2014.

(3) Sullivan, I.; Goryachev, A.; Digdaya, I. A.; Li, X.; Atwater, H. A.; Vermaas, D. A.; Xiang, C. Coupling electrochemical CO_2 conversion with CO_2 capture. *Nat. Catal.* **2021**, *4* (11), 952−958.

(4) Rogelj, J.; Huppmann, D.; Krey, V.; Riahi, K.; Clarke, L.; Gidden, M.; Nicholls, Z.; Meinshausen, M. A new scenario logic for the Paris Agreement long-term temperature goal. *Nature* **2019**, *573* (7774), 357−363.

(5) De Luna, P.; Hahn, C.; Higgins, D.; Jaffer, S. A.; Jaramillo, T. F.; Sargent, E. H. What would it take for renewably powered electrosynthesis to displace petrochemical processes? *Science* **2019**, *364* (6438), eaav3506.

(6) Keith, D. W.; Holmes, G.; St. Angelo, D.; Heidel, K. A process for capturing CO_2 from the atmosphere. *Joule* **2018**, *2* (8), 1573−1594.

(7) Welch, A. J.; Dunn, E.; DuChene, J. S.; Atwater, H. A. Bicarbonate or carbonate processes for coupling carbon dioxide capture and electrochemical conversion. *ACS Energy Lett.* **2020**, *5* (3), 940−945.

(8) Boot-Handford, M. E.; Abanades, J. C.; Anthony, E. J.; Blunt, M. J.; Brandani, S.; Mac Dowell, N.; Fernández, J. R.; Ferrari, M.-C.; Gross, R.; Hallett, J. P.; et al. Carbon capture and storage update. *Energy Environ. Sci.* **2014**, *7* (1), 130−189.

(9) Haszeldine, R. S. Carbon capture and storage: how green can black be? *Science* **2009**, *325* (5948), 1647−1652.

(10) Pérez-Gallent, E.; Vankani, C.; Sánchez-Martínez, C.; Anastasopol, A.; Goetheer, E. Integrating CO2 Capture with Electrochemical Conversion Using Amine-Based Capture Solvents as Electrolytes. *Ind. Eng. Chem. Res.* **2021**, *60* (11), 4269−4278.

(11) Lees, E. W.; Goldman, M.; Fink, A. G.; Dvorak, D. J.; Salvatore, D. A.; Zhang, Z.; Loo, N. W.; Berlinguette, C. P. Electrodes designed for converting bicarbonate into CO. *ACS Energy Lett.* **2020**, *5* (7), 2165−2173.

(12) Zhang, Z.; Lees, E. W.; Habizadeh, F.; Salvatore, D. A.; Ren, S.; Simpson, G. L.; Wheeler, D. G.; Liu, A.; Berlinguette, C. P. Porous metal electrodes enable efficient electrolysis of carbon capture solutions. *Energy Environ. Sci.* **2022**, *15* (2), 705−713.

(13) Lees, E. W.; Bui, J. C.; Song, D.; Weber, A. Z.; Berlinguette, C. P. Continuum Model to Define the Chemistry and Mass Transfer in a Bicarbonate Electrolyzer. *ACS Energy Lett.* **2022**, *7*, 834−842.

(14) Yang, K.; Li, M.; Subramanian, S.; Blommaert, M. A.; Smith, W. A.; Burdyny, T. Cation-Driven Increases of CO2 Utilization in a Bipolar Membrane Electrode Assembly for CO2 Electrolysis. *ACS Energy Lett.* **2021**, *6* (12), 4291−4298.

(15) Blommaert, M. A.; Aili, D.; Tufa, R. A.; Li, Q.; Smith, W. A.; Vermaas, D. A. Insights and Challenges for Applying Bipolar Membranes in Advanced Electrochemical Energy Systems. *ACS Energy Lett.* **2021**, *6* (7), 2539−2548.

(16) Li, T.; Lees, E. W.; Zhang, Z.; Berlinguette, C. P. Conversion of bicarbonate to formate in an electrochemical flow reactor. *ACS Energy Lett.* **2020**, *5* (8), 2624−2630.

(17) Lees, E. W.; Liu, A.; Bui, J. C.; Ren, S.; Weber, A. Z.; Berlinguette, C. P. Electrolytic Methane Production from Reactive Carbon Solutions. *ACS Energy Lett.* **2022**, *7*, 1712−1718.

(18) Kas, R.; Yang, K.; Yewale, G. P.; Crow, A.; Burdyny, T.; Smith, W. A. Modeling the Local Environment within Porous Electrode during Electrochemical Reduction of Bicarbonate. *Ind. Eng. Chem. Res.* **2022**, *61*, 10461.

(19) Kim, D.; Choi, W.; Lee, H. W.; Lee, S. Y.; Choi, Y.; Lee, D. K.; Kim, W.; Na, J.; Lee, U.; Hwang, Y. J.; et al. Electrocatalytic Reduction of Low Concentrations of CO_2 Gas in a Membrane Electrode Assembly Electrolyzer. *ACS Energy Lett.* **2021**, *6* (10), 3488−3495.

(20) Lee, G.; Li, Y. C.; Kim, J.-Y.; Peng, T.; Nam, D.-H.; Sedighian Rasouli, A.; Li, F.; Luo, M.; Ip, A. H.; Joo, Y.-C.; et al. Electrochemical upgrade of CO_2 from amine capture solution. *Nat. Energy* **2021**, *6* (1), 46−53.

(21) Chen, L.; Li, F.; Zhang, Y.; Bentley, C. L.; Horne, M.; Bond, A. M.; Zhang, J. Electrochemical reduction of carbon dioxide in a monoethanolamine capture medium. *ChemSusChem* **2017**, *10* (20), 4109−4118.

(22) Rochelle, G. T. Amine scrubbing for CO_2 capture. *Science* **2009**, *325* (5948), 1652−1654.

(23) Kim, J. H.; Jang, H.; Bak, G.; Choi, W.; Yun, H.; Lee, E.; Kim, D.; Kim, J.; Lee, S. Y.; Hwang, Y. J. Insensitive cation effect on single-atom Ni catalyst allows selective electrochemical conversion of captured CO_2 in universal media. *Energy Environ. Sci.* **2022**, *15*, 4301.

(24) Zhao, B.; Su, Y.; Tao, W.; Li, L.; Peng, Y. Post-combustion CO_2 capture by aqueous ammonia: A state-of-the-art review. *Int. J. Greenh. Gas Control.* **2012**, *9*, 355−371.

(25) Shakerian, F.; Kim, K.-H.; Szulejko, J. E.; Park, J.-W. A comparative review between amines and ammonia as sorptive media for post-combustion CO_2 capture. *Appl. Energy* **2015**, *148*, 10−22.

(26) Wang, F.; Zhao, J.; Miao, H.; Zhao, J.; Zhang, H.; Yuan, J.; Yan, J. Current status and challenges of the ammonia escape inhibition technologies in ammonia-based CO_2 capture process. *Appl. Energy* **2018**, *230*, 734−749.

(27) Echemi.com. Ammonia Market Price and Analysis. Retrieved June 11, 2022 from https://www.echemi.com/productsInformation/pid_Rock19411-ammonia.html.

(28) Echemi.com. Potassium hydroxide Market Price and Analysis. Retrieved June 11, 2022 from https://www.echemi.com/productsInformation/pd20150901020-potassium-hydroxide.html.

(29) Echemi.com. Ethanolamine Market Price and Analysis. Retrieved June 11, 2022 from https://www.echemi.com/productsInformation/pid_Seven5556-ethanolamine.html.

(30) Liu, H.; Park, J.; Chen, Y.; Qiu, Y.; Cheng, Y.; Srivastava, K.; Gu, S.; Shanks, B. H.; Roling, L. T.; Li, W. Electrocatalytic nitrate reduction on oxide-derived silver with tunable selectivity to nitrite and ammonia. *ACS Catal.* **2021**, *11* (14), 8431−8442.

(31) Daiyan, R.; Tran-Phu, T.; Kumar, P.; Iputera, K.; Tong, Z.; Leverett, J.; Khan, M. H. A.; Asghar Esmailpour, A.; Jalili, A.; Lim, M.; et al. Nitrate reduction to ammonium: from CuO defect engineering to waste NOx-to-NH_3 economic feasibility. *Energy Environ. Sci.* **2021**, *14* (6), 3588−3598.

(32) Kwon, Y.-i.; Kim, S. K.; Kim, Y. B.; Son, S. J.; Nam, G. D.; Park, H. J.; Cho, W.-C.; Yoon, H. C.; Joo, J. H. Nitric oxide utilization for ammonia production using solid electrolysis cell at atmospheric pressure. *ACS Energy Lett.* **2021**, *6* (12), 4165−4172.

(33) Kim, D.; Shin, D.; Heo, J.; Lim, H.; Lim, J.-A.; Jeong, H. M.; Kim, B.-S.; Heo, I.; Oh, I.; Lee, B.; et al. Unveiling Electrode−Electrolyte Design-Based NO Reduction for NH3 Synthesis. *ACS Energy Lett.* **2020**, *5* (11), 3647−3656.

(34) van Langevelde, P. H.; Katsounaros, I.; Koper, M. T. Electrocatalytic nitrate reduction for sustainable ammonia production. *Joule* **2021**, *5* (2), 290−294.

(35) Wang, Y.; Wang, C.; Li, M.; Yu, Y.; Zhang, B. Nitrate electroreduction: mechanism insight, in situ characterization, performance evaluation, and challenges. *Chem. Soc. Rev.* **2021**, *50* (12), 6720−6733.

(36) Jiang, K.; Li, K.; Yu, H.; Chen, Z.; Wardhaugh, L.; Feron, P. Advancement of ammonia based post-combustion CO_2 capture using the advanced flash stripper process. *Appl. Energy* **2017**, *202*, 496−506.

(37) Jiang, K.; Yu, H.; Yu, J.; Li, K. Advancement of ammonia-based post-combustion CO_2 capture technology: Process modifications. *Fuel Process. Technol.* **2020**, *210*, 106544.

(38) Hanak, D. P.; Biliyok, C.; Manovic, V. Efficiency improvements for the coal-fired power plant retrofit with CO_2 capture plant using chilled ammonia process. *Appl. Energy* **2015**, *151*, 258−272.

(39) Li, K.; Yu, H.; Yan, S.; Feron, P.; Wardhaugh, L.; Tade, M. Technoeconomic assessment of an advanced aqueous ammonia-based postcombustion capture process integrated with a 650-MW coal-fired power station. *Environ. Sci. Technol.* **2016**, *50* (19), 10746−10755.

(40) Li, K.; Yu, H.; Feron, P.; Tade, M.; Wardhaugh, L. Technical and energy performance of an advanced, aqueous ammonia-based CO_2 capture technology for a 500 MW coal-fired power station. *Environ. Sci. Technol.* **2015**, *49* (16), 10243−10252.

(41) Shin, H.; Hansen, K. U.; Jiao, F. Techno-economic assessment of low-temperature carbon dioxide electrolysis. *Nat. Sustain.* **2021**, *4* (10), 911−919.

(42) Schiffer, Z. J.; Biswas, S.; Manthiram, K. Ammonium Formate as a Safe, Energy-Dense Electrochemical Fuel Ionic Liquid. *ACS Energy Lett.* **2022**, *7*, 3260−3267.

(43) Min, X.; Kanan, M. W. Pd-catalyzed electrohydrogenation of carbon dioxide to formate: high mass activity at low overpotential and identification of the deactivation pathway. *J. Am. Chem. Soc.* **2015**, *137* (14), 4701−4708.

(44) Li, Y. C.; Lee, G.; Yuan, T.; Wang, Y.; Nam, D.-H.; Wang, Z.; García de Arquer, F. P.; Lum, Y.; Dinh, C.-T.; Voznyy, O.; et al. CO_2 electroreduction from carbonate electrolyte. *ACS Energy Lett.* **2019**, *4* (6), 1427−1431.

(45) Lee, J.; Liu, H.; Chen, Y.; Li, W. Bismuth Nanosheets Derived by In Situ Morphology Transformation of Bismuth Oxides for Selective Electrochemical CO_2 Reduction to Formate. *ACS Appl. Mater. Interfaces.* **2022**, *14* (12), 14210−14217.

(46) Han, N.; Wang, Y.; Yang, H.; Deng, J.; Wu, J.; Li, Y.; Li, Y. Ultrathin bismuth nanosheets from in situ topotactic transformation for selective electrocatalytic CO_2 reduction to formate. *Nat. Commun.* **2018**, *9* (1), 1320.

(47) Temkin, A.; Evans, S.; Manidis, T.; Campbell, C.; Naidenko, O. V. Exposure-based assessment and economic valuation of adverse birth outcomes and cancer risk due to nitrate in United States drinking water. *Environ. Res.* **2019**, *176*, 108442.

(48) Chen, Y.; Liu, H.; Ha, N.; Licht, S.; Gu, S.; Li, W. Revealing nitrogen-containing species in commercial catalysts used for ammonia electrosynthesis. *Nat. Catal.* **2020**, *3* (12), 1055−1061.

(49) National Center for Biotechnology Information. PubChem Compound Summary for CID 222, Ammonia. Retrieved May 23, 2022 from https://pubchem.ncbi.nlm.nih.gov/compound/Ammonia.

(50) Chen, Y.; Ammari-Azar, O.; Liu, H.; Lee, J.; Xi, Y.; Castellano, M.; Gu, S.; Li, W. An integrated sustainable process for economically upcycling waste nitrogen enabled by low-concentration nitrate electrodialysis and high-performance ammonia electrosynthesis. *Energy Environ. Sci.* Under Revision.